The Temperature-Composition Phase Diagram and Mesophase Structure Characterization of Monopentadecenoin in Water

Jason Briggs and Martin Caffrey
Department of Chemistry, The Ohio State University, Columbus, Ohio 43210 USA

ABSTRACT The temperature-composition phase diagram of monopentadecenoin, a monoacylglycerol with a *cis* monounsaturated fatty acid 15 carbon atoms long (C15:1c10) in water was constructed using x-ray diffraction. Low- and wide-angle diffraction patterns were collected from samples of fixed hydration as a function of temperature in the heating direction on x-ray-sensitive film. The temperature and hydration ranges investigated were 0–104°C and 0–60% (w/w) water, respectively. The phases identified in the system include the lamellar crystalline phase, the lamellar liquid crystalline phase, the fluid isotropic phase, and two inverted cubic phases belonging to space groups Ia3d (Q^{230}) and Pn3m (Q^{244}). Particular attention has been devoted to the issues of phase equilibrium, phase boundary verification, and structure characterization. The phase diagrams of monopentadecenoin, monomyristolein (C14:1c9), and monoolein (C18:1c9) are compared, and the impact of molecular structure on mesophase stability and structure is discussed.

INTRODUCTION

Lipids and lipid/water systems exhibit a rich mesomorphism. This aspect of lipid character has been investigated extensively, particularly in the past few decades. Over the years, the focus has shifted from the discovery of new liquid crystalline phases toward identifying what might be referred to as the performance characteristics of these materials in a variety of settings. Such properties as permeability and transport, water-carrying capacity, texture, bio-compatibility, and the ability to encapsulate and to effect the controlled release of water soluble and lipid soluble compounds fall under the rubric of performance characteristics.

The ability of lipids to access the liquid crystalline state is of interest to workers in a variety of disciplines, some of which include cell biology, physical chemistry and materials science. Thus, for example, we are finding that lipids, as a major component of cellular membranes, are increasingly being recognized as active participants in the functioning of this life-defining organelle and as second messengers in certain signal transduction pathways (Newton, 1993). This is in contrast to the earlier view that lipid served the subordinate role of an "inert bilayer matrix" providing support for the functionally relevant and, thus, more interesting membrane proteins (Jensen and Schutzbach, 1988; Lindblom and Rilfors, 1989; Mariani et al., 1988). The possibility of using polymerizable lipids to "lock in" technologically important structures formed by these self-assembling materials has also been investigated (Caffrey et al., 1991; Johnston et al., 1983; Takeoka et al., 1989). Others have developed templating techniques to convert lipid microstructures into more stable metalized forms for use in composite materials (Schnur, 1993). There has been a recent flurry of activity concerned with the possibility of using lipid mesophases as biocompatible encapsulating and controlled release media (Betageri and Parsons, 1992; Engstrom, 1990; Gabizon and Papahadjopoulos, 1988; Langer, 1990; Lasic et al., 1992; Puvvada et al., 1993). The explosive interest in this aspect of lipidology is evidenced not only by an increase in the number of publications in the area but also by the emergence of commercial enterprises aiming to capitalize on the pharmaceutical and/or cosmetic applicability of these most versatile of materials.

A logical approach to understanding the functioning of a complex assembly of lipid species, as is found in cellular membranes, is through the study of model systems. Further, the rational design of controlled release agents with user-defined performance characteristics can be pursued most effectively by identifying the relationship between lipid molecular structure and mesophase behavior first in simple, well defined systems. It is this relationship that we are seeking to establish in our current research program (Briggs and Caffrey, 1994). The link between molecular structure and phase behavior is being studied by comparing the temperature-composition (T-C) phase diagrams and the mesophase structure parameters for a homologous series of monoacylglycerols dispersed in water (Briggs and Caffrey, 1994). In the spirit of adding a piece to the chemical structure-mesomorphism puzzle, the T-C phase diagram of monopentadecenoin (C15:1c10 mag) in water and related structure information are presented in this paper. Monopentadecenoin contains a fatty acid chain 15 carbons atoms long, with a *cis* double bond at the 10 position, in ester linkage at the primary hydroxyl of glycerol (Fig. 1). X-Ray diffraction was used to identify and to characterize structurally the different mesophases found in the system in the temperature range of 0–104°C and in the composition range of 0–60% (w/w) water. The phase behavior and structure characteristics of monopentadecenoin are compared with and contrasted to those of related monoacylglycerols.

Received for publication 27 April 1994 and in final form 16 June 1994.
Address reprint requests to Dr. Martin Caffrey, Department of Chemistry, Ohio State University, 120 W. 18th Ave., Columbus, OH 43210. Tel.: 614-292-8437; Fax: 614-292-1532; E-mail:caffrey@osu.edu.

0006-3495/94/10/1594/09 $2.00

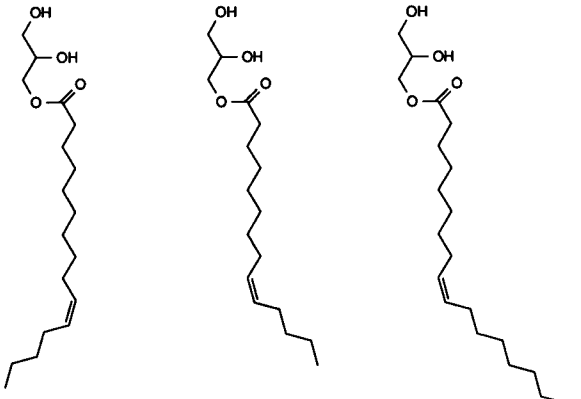

FIGURE 1 Molecular structure of the different monoacyglycerols discussed in the text.

MATERIALS AND METHODS

Pentadecenoic acid was purchased from Nu Chek Prep Inc. (Elysian, MN) and was used without further purification. All other materials were of reagent grade. Water was purified by using a Milli-Q Reagent Water System (Millipore Corporation, Bedford, MA) consisting of a carbon filter cartridge, two ion-exchange filter cartridges, and an organic removal cartridge.

Synthesis and purification

Monopentadecenoin was prepared and purified essentially as described previously for monomyristolein (Briggs and Caffrey, 1994). Specifically, two adjacent hydroxyl groups in the glycerol (2.56 g) molecule were protected from esterification by reacting with acetone (7 ml) in the presence of *p*-toluenesulfonic acid (0.15 g) and benzene (38 ml). The mixture was refluxed for 10 h using a Dean-Stark trap fitted with a water-cooled condenser and drying tube. After cooling to room temperature, 2 g of pentadecenoic acid was added and the mixture was refluxed as above for an additional 15 h. Anhydrous sodium acetate (0.2 g) was added to the flask fitted with a drying tube, and the mixture was swirled by hand for 10 min and washed 4 times with 10 ml of water (40 ml total) to remove the *p*-toluenesulfonic acid and unreacted protected glycerol. Benzene was removed by rotary evaporation after drying over anhydrous sodium sulfate. The protecting group of the esterified glycerol was removed by heating the oily product, dissolved in 2-methoxyethanol, with 5 g of boric acid in a 100-ml flask fitted with an air-cooled condenser and drying tube. The mixture was combined with 100 ml of diethyl ether and washed 4 times with 70 ml of water (280 ml total). The organic solvents were removed by rotary evaporation after drying over anhydrous sodium sulfate.

The racemic monoacylglycerol product was purified as described previously (Briggs and Caffrey, 1994) by crystallizing twice from 30 ml of 9:1 hexane/diethyl ether (v/v) cooled in a slush of chloroform and liquid nitrogen. The dried crystals were found to be >99% pure by thin layer chromatography exactly as described previously (Briggs and Caffrey, 1994), and the product yield was ~1.5 g (57%).

Spectroscopic analysis

A proton NMR spectrum of the synthesized material was collected on a Bruker AM-250, 250-MHz machine at 27°C. 15 mg of lipid was dissolved in ~0.5 ml of deuterated chloroform containing 0.03% (v/v) tetramethylsilane (Aldrich Chemical Company, Inc., Milwaukee, WI). Resonance peaks were assigned as outlined in Kates (1986). The spectrum was virtually identical to that of monomyristolein (Briggs and Caffrey, 1994). Peaks were identified in the monopentadecenoin spectrum at the chemical shift values indicated below, with the ratio of the experimental to the expected peak intensity shown in parenthesis. Peak intensities were normalized to a total nonhydroxyl proton intensity of 32. The glycerol methylene protons were observed at 3.5–4.3 ppm (5.4/5.0), the double bond protons at 5.32 ppm (1.9/2.0), the allylic methylene protons at 2.0 ppm (4.1/4.0), protons at the C2 and C3 positions of the acyl chain at 2.33 ppm (2.2/2.0) and 1.62 ppm (2.3/2.0), respectively, the terminal methyl protons at 0.9 ppm (2.8/3.0), the remaining aliphatic protons at 1.3 ppm (13.2/14.0), and the hydroxyl protons of glycerol at 2.1 ppm (2.4/2.0). There was an intense resonance at 2.15 ppm (8.1) which, most likely, is caused by a small amount of water dissolved in the deuterated chloroform. Two sharp peaks at ~1.35 and 1.41 ppm were seen with a total intensity of 2.9. These protons have been assigned to unidentified impurities.

Sample preparation

Samples of fixed hydration were prepared by mechanically mixing appropriate amounts of lipid and water to achieve the desired overall sample composition. Homogeneity was affected by cycling the lipid/water mixture between two 250 μl gas tight syringes (Hamilton Company, Reno, NV) through a short (6 mm) 22 gauge coupling needle as described previously (Briggs and Caffrey, 1994). The mixture was loaded into 3 cm long, 1.0 mm diameter quartz x-ray capillaries (Charles Supper, Natick, MA) by removing the coupler and attaching a standard 22-gauge needle to the syringe containing the sample followed by rapid delivery of the sample into the capillary. The capillaries were flame-sealed, glued with 5 min epoxy (Hardman Inc., Belleville, NJ), and stored at 4°C for 2–4 weeks before data collection. The actual composition of the samples was determined gravimetrically as described (Briggs and Caffrey, 1994)

X-ray diffraction

X-ray source

X-Ray data were collected on line X9B at the National Synchrotron Light Source (NSLS), Brookhaven National Laboratory and on a Rigaku RU-300 18 kW rotating anode x-ray generator (Rigaku USA, Inc., Danvers, MA). At NSLS, the machine energy was 2.528 GeV with an operating beam current typically between 135 and 180 mA. The x-ray beam was focused with the second of a double-bounce silicon (111) crystal monochromator and a nickel-coated aluminum mirror. The x-ray beam energy was 8 keV (1.55 Å) with a flux on the order of 10^{11} photons/s on the sample. The beam size at the sample was ~6 mm in the horizontal direction and 0.7 mm in the vertical direction. At the detector, the convergent beam measured 0.45 mm in the horizontal and 0.32 mm in the vertical directions. Typical exposure times were 15 s on x-ray-sensitive film (DEF-5, Kodak, Rochester, NY). The sample-to-film distances used ranged from 10 to 40 cm depending on the spatial resolution required.

The rotating anode source utilized a copper target and a 0.3 mm point focus cathode. The accelerating voltage was 40 kV, and the electron beam current was 100 mA. The x-ray beam was horizontally and vertically focused with a pair of nickel-coated glass mirrors (Charles Supper, Natick, MA) giving a spot size at the detector of ~0.3 mm × 0.6 mm. The mirrors were located ~30 cm downstream of the target with a 6° take-off angle. The air gap between the x-ray shutter and the mirrors was minimized with a 15 cm long vacuum flight tube fitted with 0.5 mil (0.013 mm) thick Kapton (Du Pont Electronics, Wilmington, DE) windows. X rays were directed through a 0.025 mm thick nickel filter giving a copper Kα-to-Kβ intensity ratio of ~100:1 with a total Kα transmittence of 58% (Cullity, 1978). The sample-to-film distance was determined to be ~23 cm using a sample of known d-spacing (fully hydrated dihexadecylphosphatidylethanolamine, 30°C, d = 60.8 Å, (Hogan, 1989)). Exposure times were typically 6 h on film (DEF-5, Kodak, Rochester, NY).

Data collection

Samples of monopentadecenoin, ranging from 0–60% (w/w) water, and contained in x-ray capillaries at 4°C, were placed in a multiple sample holder (Briggs and Caffrey, 1994) at 0°C. The samples were incubated for approximately 15 min at 0°C before collecting the first diffraction pattern.

Samples containing less than 30% (w/w) water were incubated for ~25 min at fixed temperatures ranging from 0–100°C, in 5°C intervals in the heating direction, before collecting the diffraction patterns. Samples containing greater than 30% (w/w) water were subjected to a 15°C/h (0.25°C/min) temperature-ramp in the range of 50–100°C. The ramp was stopped at 5°C intervals and diffraction patterns were collected after a 2 min equilibration time at each temperature. In the temperature range of 0–45°C, samples containing greater than 30% (w/w) water were incubated for a minimum of 6 h at 5°C intervals before collecting the diffraction pattern. Patterns were collected using a multiple frame/streak film device (Briggs and Caffrey, 1994). At lower temperatures and in samples containing relatively large amounts of water, changes in temperature cause large changes in phase composition. This is especially true for the cubic mesophase (Fig. 2). Accordingly, the 6 h equilibration was implemented to allow for structure relaxation in samples containing more than 30% (w/w) water and at temperatures below 45°C.

RESULTS

Phase diagram

The phases identified by x-ray diffraction and their location in temperature-composition space are shown in Fig. 2 *A*. Fig. 2 *B* shows the phase boundaries and coexistence regions based on the diffraction data. The phases found in this system include the lamellar crystalline (L_c) phase, the lamellar liquid crystalline (L_α) phase, the fluid isotropic (FI) phase, and two inverted cubic phases belonging to space groups Pn3m (Q^{224}) and Ia3d (Q^{230}). Between 0 and 40°C, an L_c phase is identified in dry lipid samples. This crystalline region contains more than a single crystal polymorph, but this aspect of dry monopentadecenoin behavior was not examined further in this study. The FI phase is formed above 40°C in dry monopentadecenoin. The melting temperature has a limiting value of ~100°C in samples containing greater than 40% (w/w) water. The L_α phase exists as a pure phase between approximately 18 and 30% (w/w) water at 0°C. Above 30°C, the pure L_α phase region is roughly triangular in shape, with the upper apex located at a temperature of ~90°C and a composition of 23% (w/w) water. A pure Ia3d phase is found in samples ranging from ~24 to 35% (w/w) water at 85°C. This pure phase region narrows to a point at ~51% (w/w) water and 38°C. The pure Pn3m phase is identified between 33 and 37% (w/w) water at 95°C and above 55% (w/w) water at 35°C. The hydration limit of the Pn3m phase was not determined below 50°C because of the weakness of the diffraction pattern in the corresponding composition range.

At hydration levels greater than ~30% (w/w) water and at temperatures below 30°C, the fully hydrated L_α phase coexists with an excess water phase. The L_α and Ia3d phases coexist between roughly 29 and 49% (w/w) water at 40°C.

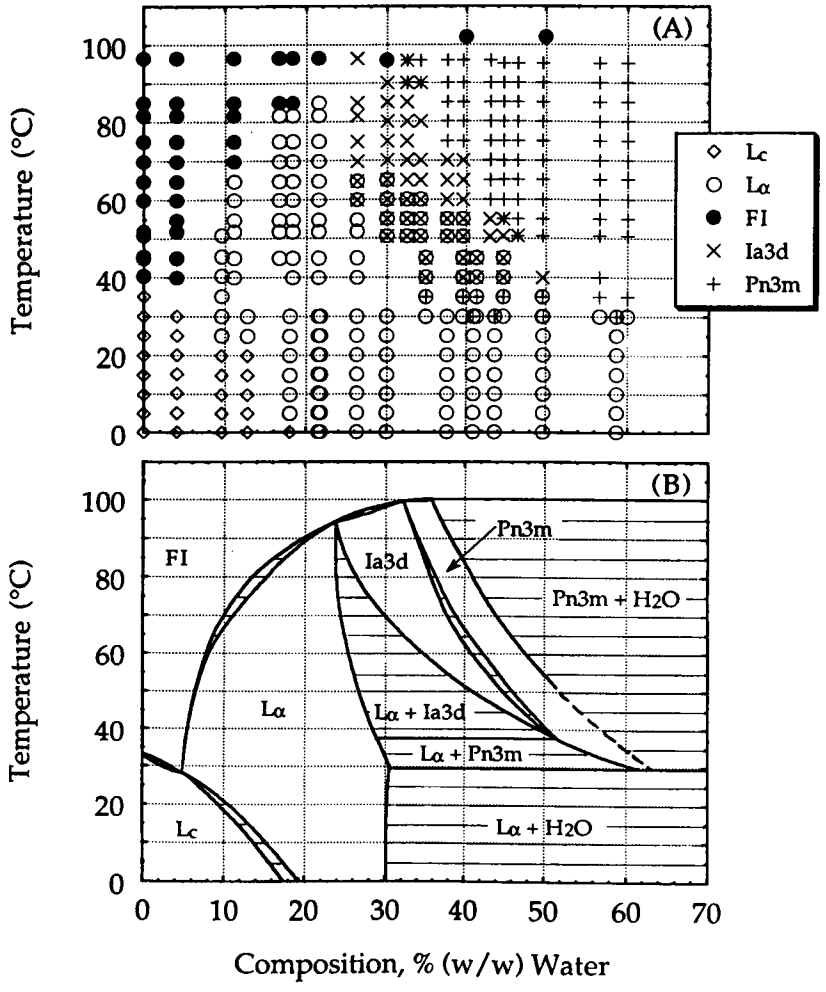

FIGURE 2 (*A*) Identity and location in temperature-composition space of each phase and coexisting phases in the monopentadecenoin/water system as determined by x-ray diffraction in the heating direction. (*B*) Temperature-composition phase diagram of the monopentadecenoin/water system based on an interpretation of the data in *A*. The hydration boundary of the L_α phase, below 30°C, was taken as the composition at which the addition of water to the lipid sample did not result in an increase in the repeat spacing of the lamellar phase (data not shown). The cubic phase hydration boundary was estimated and verified as described under Results.

This coexistence region has an upper temperature limit of 89°C observed at 23% (w/w) water. The L_α and Pn3m phases coexist in the composition range of ~30–61% (w/w) water at 30°C, whereas at 38°C coexistence extends from ~29 to 51% (w/w) water.

Mesophase expansion coefficients

The temperature- and composition dependence of the unit cell dimension of the different mesophases present in the phase diagram above are shown in Figs. 3 and 4, respectively. Without exception, the lattice parameter of all liquid crystalline phases examined decreases with increasing temperature (Fig. 3). Additionally, the lattice parameter of the pure mesophases increases with sample hydration (Fig. 4). These dependencies are conveniently quantified as the thermal and compositional expansion coefficients α and β, respectively, defined as follows (Briggs and Caffrey, 1994):

$$\alpha = (1/\eta)(\Delta\eta/\Delta T) \quad (1)$$

and

$$\beta = (1/\eta)(\Delta\eta/\Delta W), \quad (2)$$

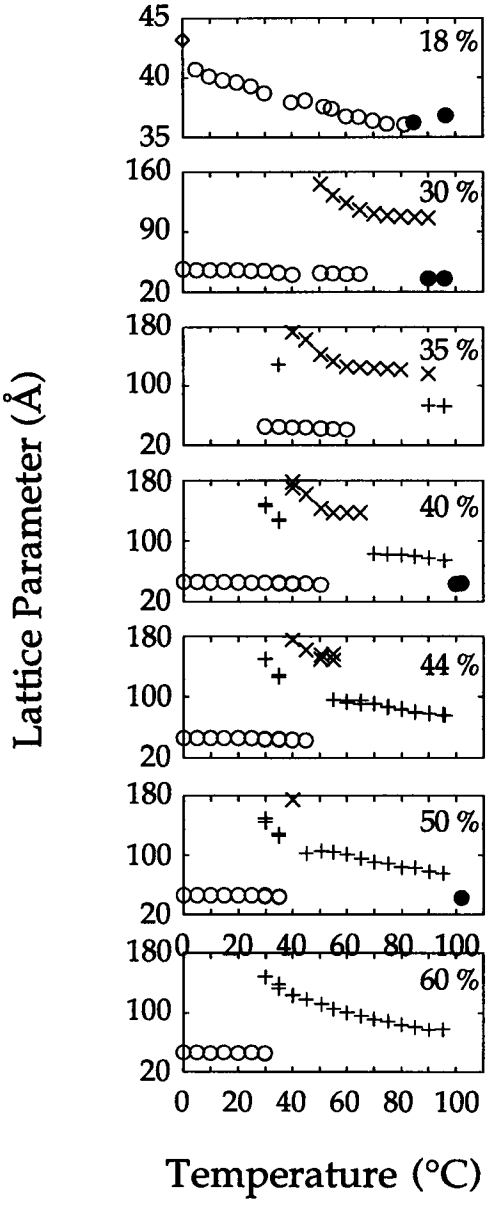

FIGURE 3 Temperature dependence of the lattice parameters of the phases found in the monopentadecenoin/water system at the indicated overall sample compositions in units of % (w/w) water. The identity of the phases is as follows: (●) FI, (◇) L_c, (○) L_α, (×) Ia3d, and (+) Pn3m.

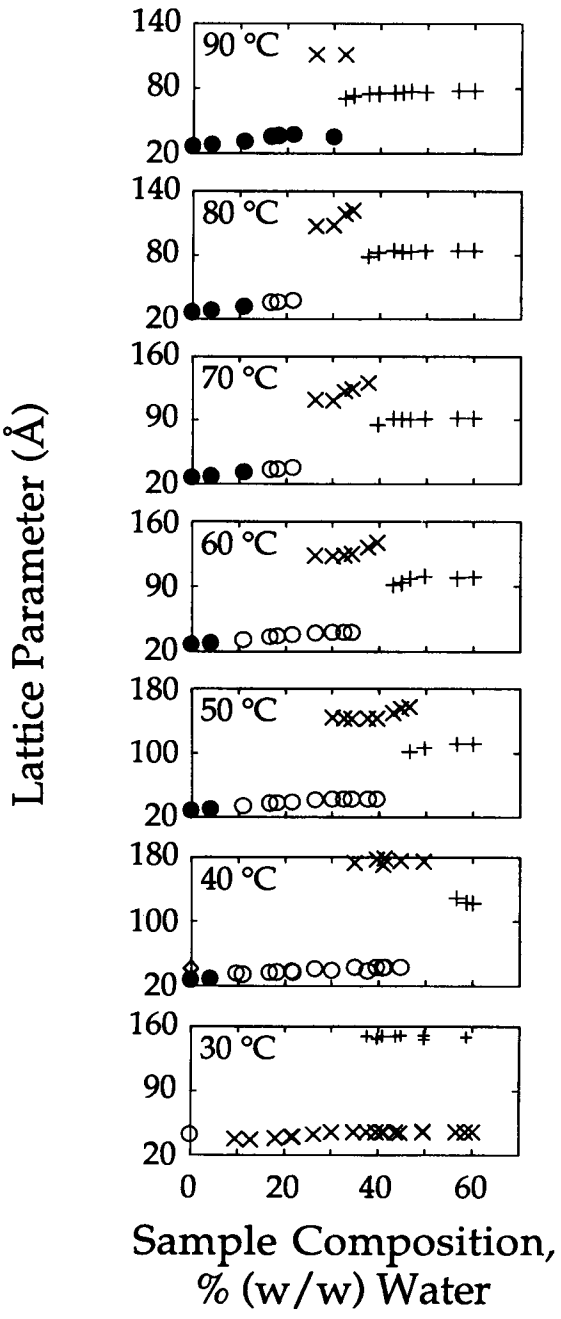

FIGURE 4 Composition dependence of the lattice parameters of the phases found in the monopentadecenoin/water system at selected sample temperatures. The identity of the phases is as follows: (●) FI, (◇) L_c, (○) L_α (×) Ia3d, and (+) Pn3m.

TABLE 1 Values of and parameters used in determining the thermal expansion coefficients of the different phases in the monopentadecenoin/water system

Phase	Composition, % (w/w) water	Temperature (°C)*	Equation of best fit‡	η (Å)§	α (kK^{-1})‖
L_α (pure)	18	40 (0–85)	$d = 40.4–0.0556T$ (0.9888)	38.2	−1.46
Ia3d (pure)	30	80 (75–85)	$d = 119.4–0.1465T$ (0.9977)	107.7	−1.36
Pn3m (pure)	40	75 (70–80)	$d = 94.1–0.1421T$ (0.9741)	83.4	−1.70
Ia3d ($+L_\alpha$)	30	58 (50–65)	$d = 246.0–2.0308T$ (0.9916)	128.2	−15.8
Pn3m ($+L_\alpha$)	40	30 (30–35)	$d = 263.1–3.8840T$ (1)	146.5	−26.5

* Temperature at which the thermal expansion coefficient was evaluated. The temperature range ($T_1 - T_2$) over which the temperature dependence of the lattice parameter was fit is indicated in parenthesis.

‡ Equation of the straight line best describing the temperature dependence of the lattice parameter in the range indicated. The units of d and T are Å and °C, respectively. The correlation coefficient, R, of the fitted line is shown in parenthesis.

§ η is the lattice parameter calculated at the temperature indicated and used in determining the thermal expansion coefficient.

‖ The thermal expansion coefficient α is defined as $(1/\eta)(\Delta\eta/\Delta T)$, where $\Delta T = T_2 - T_1$ and kK^{-1} = kilo K^{-1}.

where $\Delta\eta/\Delta T$ and $\Delta\eta/\Delta W$ represent the slope of a straight line fit to the temperature- and composition dependence of the lattice parameters of the different phases over a limited temperature or composition range, respectively. η is the lattice parameter of the phase calculated from the equation of the aforementioned fitted line at a specified temperature or composition. The thermal expansion coefficients range from -1 kK^{-1} to -2 kK^{-1} for the pure phases and -15 kK^{-1} to -27 kK^{-1} for cubic phases that are coexistence with the L_α phase (Table 1). The compositional expansion coefficients have values ranging from 124 to 205 ppm^{-1} (Table 2). These values are typical of what was seen for the mesophases identified in the homologous monomyristolein/water system (Briggs and Caffrey, 1994).

Cubic phase boundary verification

The phase boundaries in the monopentadecenoin phase diagram (Fig. 2 *B*) were drawn based solely on the identification of pure phase regions and regions of phase coexistence at specific temperatures and sample compositions using x-ray diffraction (Fig. 2 *A*). The position of the hand-drawn cubic phase boundaries was verified as described previously (Briggs and Caffrey, 1994). Briefly, lipid length, l, was calculated for the *pure* cubic phase by using the lattice parameter, a, determined by x-ray diffraction, the known sample composition, Φ_l, and by using the following relation (Turner et al., 1992):

$$\Phi_l = 2A_0\left(\frac{l}{a}\right) + \frac{4\pi\chi}{3}\left(\frac{l}{a}\right)^3, \quad (3)$$

where A_0 and χ are constants having values specific to the different cubic phases (Ia3d: $A_0 = 3.091$, $\chi = -8$; Pn3m: $A_0 = 1.919$, $\chi = -2$) (Anderson et al., 1989). l is assumed to be independent of composition and cubic phase type (Chung and Caffrey, 1994; Turner et al., 1992). The values of l, calculated for the pure cubic phases over a range of composition, have been plotted against temperature (Fig. 5), and the corresponding data were fit with the following exponential (correlation coefficient = 0.798):

$$l = 16e^{(-0.0019T)}, \quad (4)$$

where T and l have units of °C and Å, respectively. Equation 4 was used to assign values of l to cubic phases *in a two-phase coexistence region* at a specific temperature (Briggs and Caffrey, 1994). The assigned l value, together with the a value obtained by x-ray diffraction in the two-phase region, were combined in Eq. 3 to determine the corresponding Φ_l value of the cubic phase in the two-phase region. The calculated cubic phase composition, Φ_l, gives the position of the cubic phase boundary at that temperature. When more than one diffraction measurement was made along a single isotherm within a two-phase region, the mean calculated cubic

TABLE 2 Values of and parameters used in determining the compositional expansion coefficients of the different phases in the monopentadecenoin/water system

Phase	Temperature (°C)	Composition, % (w/w) water*	Equation of best fit‡	η (Å)§	β (ppm^{-1})‖
L_α	25	15 (10–30)	$d = 30.7 + 0.4694W$ (0.9929)	37.7	124
Ia3d	50	43 (41–43)	$d = 18.0 + 3.0765W$ (1)	150.3	205
Pn3m	60	45 (41–45)	$d = 13.4 + 1.8307W$ (0.9834)	95.8	191

* Sample composition at which the compositional expansion coefficient was evaluated. The composition range ($C_1 - C_2$) over which the composition dependence of the lattice parameter was fit is indicated in parenthesis.

‡ Equation of the straight line best describing the composition dependence of the lattice parameter in the range indicated. The units of d and W are Å and % (w/w) water, respectively.

§ η is the lattice parameter calculated at the composition indicated and used in determining the compositional expansion coefficient.

‖ The compositional expansion coefficient β is defined as $(1/\eta)(\Delta\eta/\Delta W)$, where $\Delta W = C_2 - C_1$ and ppm^{-1} is [parts per million (w/w) water]$^{-1}$.

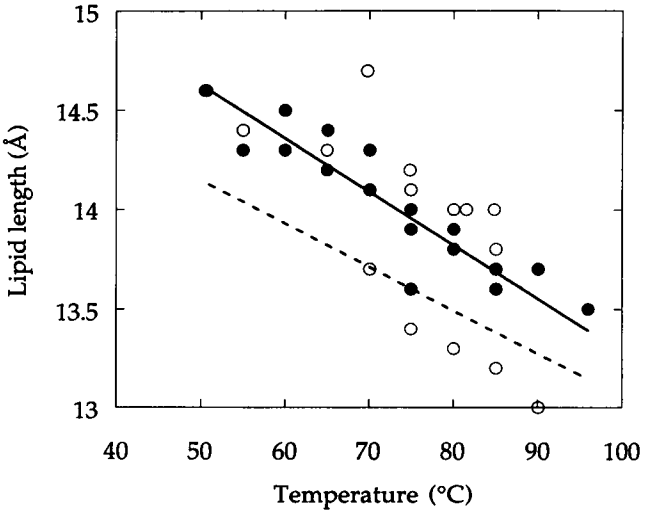

FIGURE 5 Temperature dependence of the lipid length, l, calculated for the pure cubic phases found in the monopentadecenoin system using Eq. 1. The data were fit with the following exponential: $l = 16.12e^{(-0.00197)}$, where T is temperature in °C and l is in Å (——). The correlation coefficient was 0.798. Solid and open circles correspond to the Ia3d and Pn3m phases, respectively. The six data points that lie conspicuously below the fitted line are from a single sample. An error in the gravimetrically determined composition of this sample would account for the displacement of this set of data points. These data were included in the fit, however. The dashed line is the exponential fit of l versus temperature [$l = 15e^{(-0.00167)}$] for the cubic phases of monomyristolein taken from Briggs and Caffrey (1994). See text for details.

phase composition was taken as the boundary position. Following this approach to phase boundary verification, the data in Table 3 show that the hand drawn and calculated phase boundaries agree to within ±1.5% (w/w) water in most cases.

TABLE 3 Calculated and estimated cubic phase boundaries in the temperature-composition phase diagram of the monopentadecenoin/water system

Temperature (°C)	Phase boundary*	Composition at boundary, % (w/w) water	
		Estimated‡	Calculated§
30	L_α + Pn3m/Pn3m	61	61.62 ± 0.42 (8)
35	L_α + Pn3m/Pn3m	55	56.26 ± 0.42 (8)
40	L_α + Ia3d/Ia3d	49	49.20 ± 0.80 (4)
45	L_α + Ia3d/Ia3d	45	46.28 ± 0.10 (3)
50	L_α + Ia3d/Ia3D	41	40.57 ± 0.32 (5)
50	Ia3d/Ia3d + Pn3m	45	45.29 (1)
50	Ia3d + Pn3m/Pn3m	46	47.37 (1)
50	Pn3m/Pn3m + H_2O	52	51.76 ± 0.04 (2)
55	L_α + Ia3d/Ia3d	37	36.99 ± 0.29 (4)
55	Ia3d/Ia3d + Pn3m	43	45.32 (1)
55	Ia3d + Pn3m/Pn3m	44	45.24 (1)
55	Pn3m/Pn3m + H_2O	50	49.03 ± 0.32 (3)
60	L_α + Ia3d/Ia3d	34	33.88 ± 0.44 (4)
60	Pn3m/Pn3m + H_2O	47	47.62 ± 0.43 (3)
65	L_α + Ia3d/Ia3d	32	30.53 ± 0.89 (2)
65	Pn3m/Pn3m + H_2O	46	45.59 ± 0.28 (5)
70	Pn3m/Pn3m + H_2O	44	43.79 ± 0.34 (6)
75	Pn3m/Pn3m + H_2O	42	42.68 ± 0.69 (6)
80	Pn3m/Pn3m + H_2O	41	40.60 ± 0.28 (6)
85	Pn3m/Pn3m + H_2O	40	39.29 ± 0.97 (7)
90	Ia3d/Ia3d + Pn3m	34	32.90 ± 0.93 (2)
90	Ia3d + Pn3m/Pn3m	34	34.45 ± 1.10 (2)
90	Pn3m/Pn3m + H_2O	38	38.18 ± 0.42 (8)
95	Ia3d/Ia3d + Pn3m	33	31.41 (1)
95	Ia3d + Pn3m/Pn3m	33	33.32 (1)
95	Pn3m/Pn3m + H_2O	37	37.37 ± 0.68 (8)

* The phase boundary under consideration in each table entry is represented by the "/" symbol. Where a two phase region was encountered, the coexisting phases are indicated by a "+" sign.
‡ The estimated position of the phase boundaries corresponds to the hand-drawn boundary lines based on the identification of pure phase regions and regions of phase coexistence by x-ray diffraction (Materials and Methods).
§ Values represent averages ±1 SD with the number of data points used in the average calculation shown in parenthesis.

DISCUSSION

Equilibrium

Our primary objective in performing the detailed analysis reported above under Results was to verify that the T-C phase diagram constructed on the basis of diffraction measurements (Fig. 2) represented the equilibrium behavior of the monopentadecenoin/water system. Adherence to the Gibbs phase rule (Gibbs, 1878) and to the lever rule was used as criteria for evaluating equilibrium behavior. The phase rule, as applied to this two component system at constant pressure, can be written in the form

$$3 - P = F, \quad (5)$$

where P is the number of phases that can coexist at equilibrium and F is the variance or the number of intensive variables, in this case phase composition and temperature (Atkins, 1982). According to Eq. 5, the maximum number of phases that can coexist under equilibrium conditions is three. In this case F is zero, meaning that three phases of defined composition can coexist only at a single temperature. A four phase coexistence region would be in violation of the phase rule and would suggest nonequilibrium behavior. No such region was found by x-ray diffraction anywhere in the monopentadecenoin phase diagram (Fig. 2). Additionally, all three-phase regions in Fig. 2 are present either as points at the intersection of three single phase regions or as horizontal boundaries separating two two-phase regions. A triple point is located, for example, at the intersection of the FI, L_α, and Ia3d phases. A three-phase line separates the L_α+Ia3d and the L_α+Pn3m phase coexistence regions. The three phase lines must be horizontal to comply with Eq. 5 (Atkins, 1982). Indeed, this is the case with the monopentadecenoin phase diagram to within the resolution of our measurements (Fig. 2).

The lever rule, used as the second test of equilibrium behavior, describes how the relative amounts and the composition of coexisting phases change as a two phase region is traversed in temperature and/or composition (Atkins, 1982). At a fixed temperature, the composition of two coexisting phases is required to remain constant, while the relative amounts of the two phases change, as the overall sample composition is varied. This consequence of the lever rule should be reflected in the current system as constant lattice parameters for each of two coexisting phases while overall sample hydration is changed isothermally. Such behavior is

clearly demonstrated in Fig. 4. Thus, for example, along the 50°C isotherm, the L_α and Ia3d lattice parameters remain constant at 42.3 and 143.6 Å, respectively, throughout the two phase coexistence region in the range of 30–40% (w/w) water. Consistency with the lever rule is apparent along several other isotherms in Fig. 4.

The relationship between the slope of a particular phase boundary and the temperature dependence of the lattice parameters of two coexisting phases has been described previously (Briggs and Caffrey, 1994). In short, a relatively large adjustment in phase hydration is suggested when the lattice parameter of one of the phases in a two phase region is particularly sensitive to temperature. This should be reflected in the phase diagram as a gently sloping phase boundary. Conversely, if the lattice parameter of a particular phase in a two-phase region is relatively temperature-insensitive, little adjustment in phase hydration is expected to accompany the temperature change. A more vertically sloped phase boundary is expected in this case.

Several of the features identified in the last paragraph are illustrated by the data in Fig. 3. For example, as the sample containing 30% (w/w) water was heated from 50 to 65°C, the lamellar repeat spacing of the L_α phase decreases from 42 to 40 Å. In this same temperature range, the lattice of the coexisting Ia3d phase contracts by 30 from 145 to 115 Å. The small change in the L_α phase lattice size suggests that the phase composition remains relatively constant during heating. Accordingly, the boundary separating the L_α phase from the L_α+Ia3d phase coexistence region should be nearly vertical in this temperature range. The temperature dependence data above also suggest that the boundary between the L_α+Ia3d coexistence region and the pure Ia3d phase is much more gently sloped. This is precisely what is found in the corresponding phase diagram (Fig. 2 *B*). Several other examples of this kind of behavior can be found by comparing the data in Figs. 2 and 3.

The observation that the data in Fig. 2 are in agreement with the phase rule and the lever rule, plus the fact that the phase boundary slopes are consistent with the temperature-dependent changes in phase lattice parameters (Fig. 3) corroborate the view that equilibrium behavior prevails in the monopentadecenoin/water T-C phase diagram shown in Fig. 2.

Related systems

At first glance, the phase diagram of monopentadecenoin in water (Fig. 2) does not differ greatly from that of its homolog, monomyristolein (Fig. 6 (Briggs and Caffrey, 1994)). There are, however, subtle and important differences between the two that can be understood in the context of the different molecular structures involved. Monomyristolein incorporates a fatty acid that is 14 carbon atoms long with a *cis*-double bond at the 9 position (Fig. 1). In contrast, the double-bond of monopentadecenoin is located at carbon 10 on a 15 carbon atom long acyl chain.

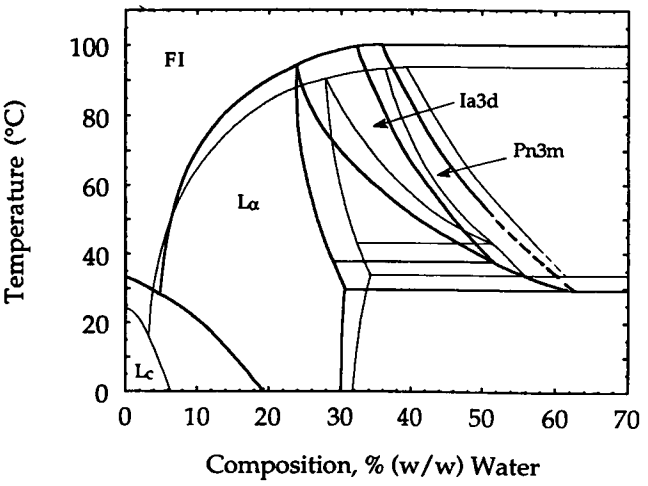

FIGURE 6 An overlay of the temperature-composition phase diagrams of the monomyristolein/water (Briggs and Caffrey, 1994, narrow lines) and monopentadecenoin/water systems (this work, *bold lines*).

The melting point of the dry monoacylglycerol is ~10°C higher in the longer chained lipid, which undergoes an L_c-to-FI transition at 40°C (Fig. 2). In monomyristolein, the dry material is completely melted at 30°C (Fig. 6). This chain length-dependent increase in melting temperature is seen in many lipid classes including n-alkanes, fatty acids, triacylglycerols (Small, 1986), and certain phospholipids (Koynova and Caffrey, 1994). Interestingly, the L_c phase is stable up to a sample hydration value of 18% (w/w) water at 0°C in the monopentadecenoin system, whereas with monomyristolein the lyotropic L_c-to-L_α phase transition has already taken place at a hydration value of 8% (w/w) water at this same temperature. It would appear, therefore, that slight differences in chain structure can profoundly alter the stability of the crystalline phase(s).

The fact that chain shortening stabilizes the lamellar phases relative to the non-lamellar phases in monoacyglycerols has been discussed previously (Briggs and Caffrey, 1994). This trend is observable *even with a chain length difference of one carbon atom.* In the monopentadecenoin phase diagram, the Ia3d and Pn3m phases exist down to temperatures of 38 and 30°C, respectively. The corresponding phase boundaries in the monomyristolein system are found at 42 and 35°C (Fig. 6). Additionally, both cubic phases appear at lower hydration values, regardless of temperature, in the monopentadecenoin phase diagram than in that of monomyristolein. In the phase diagram of monoolein (not shown), a monoacylglycerol homolog with a chain length of 18 carbon atoms and a *cis* double bond at position 9 (Fig. 1), the cubic phases are stable down to at least 20°C (Hyde et al., 1984). Taken together, these data show that the nonlamellar phases occupy a greater area of temperature-composition space, at the expense of the L_α phase, as the acyl chain is lengthened. In general, phase boundaries in the phase diagram of monopentadecenoin lie at intermediate positions between those of monomyristolein and monoolein, with closest resemblance to the former.

So far, the discussion has dealt with the issue of chain length without regard to the change in position of the double bond in going from monopentadecenoin to monomyristolein and monoolein. Both monomyristolein and monoolein have a *cis*-double bond at carbon 9, whereas the corresponding position in monopentadecenoin is at carbon atom 10. It is useful to note that although the double bond in both monomyristolein and monoolein is at the 9 position, it is merely a consequence of nomenclature that locates this bond at the "same" position in the two structures. For purposes of discussion, let us define a relative double bond position as the ratio of the position of the double bond in the acyl chain, in terms of number of carbon atoms up to and including the carbonyl carbon, to the total number of carbon atoms in the chain. Thus, the relative position of the double-bond in monomyristolein, monopentadecenoin, and monoolein is (9/14 =) 0.64, (10/15 =) 0.67, and (9/18 =) 0.5, respectively. What, if any, is the significance of this change in relative double bond position? Our limited data set of three phase diagrams does not allow us to answer the question satisfactorily at this time. However, we are intent on determining the separate influences of chain length and double-bond position on the structure-mesophase relationship by comparing the phase behavior of a series of monoacylglycerols where the relative position of the double bond remains fixed, as in the series C14:1c7, C16:1c8, C18:1c9, C20:1c10 to that of a series such as C14:1c9, C16:1c9, C18:1c9, C20:1c9, where the site of unsaturation relative to the carbonyl carbon does not change.

Structure parameters

The comparison above focused on the relative stability of the different mesophases in temperature-composition space as influenced by the structure of the acyl chain. The data we have collected in the course of this study allow us to establish the effect of chain identity on the structure parameters within a given phase. Table 4 shows a comparison of the lattice parameters of the different mesophases found in the monopentadecenoin (this work) and monomyristolein (Briggs and Caffrey, 1994) systems at similar temperatures and degrees of hydration. The data show that there is a consistent decrease, on the order of a few ångströms, in the lattice size of the L_α, Ia3d, and Pn3m phases that accompanies the change from monopentadecenoin to monomyristolein. This is a reasonable result in that the effective length of a methylene group in the fully hydrated L_α phase of phosphatidylethanolamines measured at 3°C above the lamellar chain order/disorder transition temperature is 0.74 Å (Seddon et al., 1984). In lamellar crystalline phases, the corresponding contribution is 1.27 Å (Small, 1986). The average decrease in the L_α phase lamellar repeat spacing upon changing structure from monopentadecenoin to monomyristolein is ~2 Å (Table 4). This corresponds to a 1-Å contraction per lipid monolayer in the repeat unit and is slightly higher than the literature value cited above. The difference may be accounted for by the fact that the monoacylglycerol measurements were made under water-stressed conditions while the phosphatidylethanolamine study was performed in an excess of water.

The change from monopentadecenoin to monomyristolein results in a decrease of ~0.4 Å in the lipid length, *l*, calculated for the corresponding pure cubic phases at temperatures between 50 and 90°C (Fig. 5). This change in *l* is manifested as an average decrease in the measured cubic phase lattice parameter of 2 Å (Table 4).

The temperature dependence of the calculated lipid length in the cubic mesophase is approximately linear in the 50–90°C range studied (Fig. 5). In this range, the value of *l* decreases by ~1 Å. A similar change is seen for the cubic phases of monomyristolein (Fig. 5) and monoolein (data not shown), and for the interaxial lipid monolayer thickness of the inverted hexagonal phase of hydrated 1,2-dioleoyl-*sn*-glycero-3-phosphocholine (DOPE) (Tate and Gruner, 1989).

TABLE 4 Comparison of the structure parameters of hydrated monomyristolein (MM) and monopentadecenoin (MP) under identical conditions of temperature and composition

Phase	Composition, % (w/w) water	Temperature (°C)	Lattice parameter (Å)*		Difference (Å)
			MM	MP	
L_α	18	20	36.7 ± 0.03 (4)	39.2 ± 0.10 (3)	2.5 ± 0.13
		50	35.1 ± 0.06 (2)	37.6 ± 0.40	2.5 ± 0.46
		80	34.8 ± 0.25 (2)	36.1 ± 0.40	1.3 ± 0.65
Ia3d	32	75	115.8 ± 1.0	119.5 ± 0.95 (6)	3.7 ± 1.95
		80	115.1 ± 1.0	118.8 ± 0.21 (4)	3.7 ± 1.21
		85	115.2 ± 1.0	116.8 ± 0.06 (2)	1.6 ± 1.06
Pn3m	38	80	78.6 ± 1.5	79.2 ± 1.1 (4)	0.6 ± 2.60
		85	77.6 ± 1.5	78.8 ± 0.82 (3)	1.2 ± 2.32
		90	77.0 ± 1.5	78.9 ± 0.92 (3)	1.9 ± 2.42

* Lattice parameters for monomyristolein are from a separate study (Briggs and Caffrey, 1994). Errors in the lattice parameter indicate 1 SD in the average value calculated from the number of reflections, shown in parenthesis, recorded in a single x-ray diffraction pattern. For the cubic phases of monomyristolein, an error of 1 pixel, corresponding to 97.6 μm, was estimated in the measured radius of the lowest angle reflection of the x-ray diffraction pattern as collected on image plates (Briggs and Caffrey, 1994). Similarly, the maximum error in measuring the diameter of the (001) reflection of the L_α phase in monopentadecenoin at 50 and 80°C, where only one reflection was recorded, was estimated to be 0.5 mm. The corresponding errors in lattice parameter are indicated in the table.

To a first approximation, it would appear as though the thermal expansion properties of lipid length in inverted mesophases is relatively insensitive to chemical structure and, indeed, to mesophase identity. A more complete evaluation of these observations and their general applicability awaits the construction of the T-C phase diagrams and structural characterization of a series of monoacylglycerols dispersed in water. This represents work in progress.

CONCLUSION

The temperature-composition phase diagram of monopentadecenoin in water was presented. The behavior of monopentadecenoin was compared with that of the related monoacylglycerols, monoolein and monomyristolein, both in terms of phase stability and structure parameters of the different phases as determined by x-ray diffraction. Lengthening the acyl chain by as little as one carbon atom had the anticipated effect of enhancing the stability of nonlamellar relative to lamellar phases. The chain length increase was manifested as a 1–4 Å increase in the lattice parameter of the different mesophases under identical conditions of temperature and hydration.

Although a relationship has been shown to exist between lipid molecular structure and mesophase behavior, it is expected that mesophase structural features will dictate the performance characteristics of any system incorporating these liquid crystalline phases. The identification of such relationships in an appropriately chosen set of lipids will provide a set of rules that can be used in the rational design of systems with user-defined properties. Systematic studies continue to be carried out in this laboratory in the spirit of contributing to the establishment of these rules.

We thank the staff at the X9B line of NSLS (DOE grant KP04-01 and -B043) for their help and support. We also thank J. Ahn, A. Cheng, H. Chung, H. Kim, S. Kirchner, J. Wang, Z. Yin, and T. Zhu for valuable discussions and critical evaluation of this manuscript.

This work was supported by a Dow Cooperative Research Program Award (The Dow Chemical Company) and grants from the National Institutes of Health (DK 36849 and DK 45295) and the National Science Foundation (DIR 9016683).

REFERENCES

Anderson, D., H. Wennerstrom, and U. Olsson. 1989. Isotropic bicontinuous solutions in surfactant-solvent systems: the L_3 phase. *J. Phys. Chem.* 93:4243–4253.

Atkins, P. W. 1982. Physical Chemistry. W. H. Freeman and Co., San Francisco, CA. 1095 pp.

Betageri, G., and D. Parsons. 1992. Drug encapsulation and release from multilamellar and unilamellar liposomes. *Int. J. Pharmacol.* 81:235–241.

Briggs, J., and M. Caffrey. 1994. The temperature-composition phase diagram of monomyristolein in water: equilibrium and metastability aspects. *Biophys. J.* 66:573–587.

Caffrey, M., A. Rudolph, and J. Hogan. 1991. Diacetylenic lipid microstructures: structural characterization by x-ray diffraction and comparison with the saturated phosphatidylcholine analogue. *Biochemistry.* 30: 2134–2146.

Chung, H., and M. Caffrey. 1994. The neutral area surface of the cubic mesophase: location and properties. *Biophys. J.* 66:377–381.

Cullity, B. D. 1978. Elements of X-Ray Diffraction. Addison-Wesley, Reading, MA. 555 pp.

Engstrom, S. 1990. Cubic phases as drug delivery systems. *Polymer Prep.* 31:157–158.

Gabizon, A., and D. Papahadjopoulos. 1988. Liposome formulations with prolonged circulation time in blood and enhanced uptake by tumors. *Proc. Natl. Acad. Sci. USA.* 85:6949–6953.

Gibbs, J. W. 1878. On the equilibrium of heterogeneous substances. *Trans. Conn. Acad. Sci.* 3:108–248.

Hogan, J. L. 1989. Ph.D. Thesis, University of Southampton, UK.

Hyde, S., S. Andersson, B. Ericsson, and K. Larsson. 1984. A cubic structure consisting of a lipid bilayer forming an infinite periodic minimum surface of the gyroid type in the glycerolmonooleat-water system. *Z. Kristallogr.* 168:213–219.

Jensen, J., and J. Schutzbach. 1988. Modulation of dolichylphosphomannose synthase activity by changes in the lipid environment of the enzyme. *Biochemistry.* 27:6315–6320.

Johnston, D., L. McLean, M. Whitam, A. Clark, and D. Chapman. 1983. Spectra and physical properties of liposomes and monolayers of polymerizable phospholipids containing diacetylene groups in one or both acyl chains. *Biochemistry.* 22:3194–3202.

Kates, M. 1986. Techniques of Lipidology: Isolation, Analysis and Identification of Lipids. Elsevier Science Publishers B. V., Amsterdam. 464 pp.

Koynova, R., and M. Caffrey. 1994. Phases and phase transitions of the hydrated phospatidylethanolamines. *Chem. Phys. Lipids.* 69:1–34.

Langer, R. 1990. New methods of drug delivery. *Science.* 249:1527–1533.

Lasic, D., P. Frederik, M. Stuart, Y. Barenholz, and T. McIntosh. 1992. Gelation of liposome interior: a novel method for drug encapsulation. *FEBS Lett.* 312:255–258.

Lindblom, G., and L. Rilfors. 1989. Cubic phases and isotropic structures formed by membrane lipids-possible biological relevance. *Biochim. Biophys. Acta.* 988:221–256.

Mariani, P., V. Luzzati, and H. Delacroix. 1988. Cubic phases of lipid-containing systems. Structure analysis and biological implications. *J. Mol. Biol.* 204:165–189.

Newton, A. C. 1993. Interaction of proteins with lipid headgroups: lessons from protein kinase c. *Annu. Rev. Biophys. Biomol. Struct.* 22: 1–25.

Puvvada, S., S. Qadri, J. Naciri, and B. Ratna. 1993. Ionotropic gelation in a bicontinuous cubic phase. *J. Phys. Chem.* 97:11103–11107.

Schnur, J. M. 1993. Lipid tubules: a paradigm for molecularly engineered structures. *Science.* 262:1669–1676.

Seddon, J. M., G. Cevc, R. D. Kaye, and D. Marsh. 1984. X-ray diffraction study of the polymorphism of hydrated diacyl- and dialkylphosphatidylethanolamines. *Biochemistry.* 23:2634–2644.

Small, D. M. 1986. The Physical Chemistry of Lipids, From Alkanes to Phospholipids. Plenum Press, New York. 672 pp.

Takeoka, S., H. Ohno, N. Hayashi, and E. Tsuchida. 1989. Control of release of encapsulated molecules from polymerized mixed liposomes induced by physical or chemical stimuli. *J. Controlled Release.* 9:177–186.

Tate, M. W., and S. M. Gruner. 1989. Temperature dependence of the structural dimensions of the inverted hexagonal (H_{II}) phase of phosphatidylethanolamine-containing membranes. *Biochemistry.* 28:4245–4253.

Turner, D., Z.-G. Wang, S. Gruner, D. Mannock, and R. McElhaney. 1992. Structural study of the inverted cubic phases of di-dodecyl alkyl-β-D-glucopyranosyl-*rac*-glycerol. *J. Phys. II France.* 2:2039–2063.